Available online at www.sciencedirect.com
ScienceDirect
Advances in Space Research 42 (2008) 455–466
ADVANCES IN SPACE RESEARCH (a COSPAR publication)
www.elsevier.com/locate/asr

Launch of the space experiment PAMELA

M. Casolino [a,*], P. Picozza [a], F. Altamura [a], A. Basili [a], N. De Simone [a], V. Di Felice [a], M.P. De Pascale [a], L. Marcelli [a], M. Minori [a], M. Nagni [a], R. Sparvoli [a], A.M. Galper [b], V.V. Mikhailov [b], M.F. Runtso [b], S.A. Voronov [b], Y.T. Yurkin [b], V.G. Zverev [b], G. Castellini [c], O. Adriani [d], L. Bonechi [d], M. Bongi [d], E. Taddei [d], E. Vannuccini [d], D. Fedele [d], P. Papini [d], S.B. Ricciarini [d], P. Spillantini [d], M. Ambriola [e], F. Cafagna [e], C. De Marzo [e,†], G.C. Barbarino [f], D. Campana [f], G. De Rosa [f], G. Osteria [f], S. Russo [f], G.A. Bazilevskaja [g], A.N. Kvashnin [g], O. Maksumov [g], S. Misin [g], Yu.I. Stozhkov [g], E.A. Bogomolov [h], S.Yu. Krutkov [h], N.N. Nikonov [h], V. Bonvicini [i], M. Boezio [i], J. Lundquist [i], E. Mocchiutti [i], A. Vacchi [i], G. Zampa [i], N. Zampa [i], L. Bongiorno [j], M. Ricci [j], P. Carlson [k], P. Hofverberg [k], J. Lund [k], S. Orsi [k], M. Pearce [k], W. Menn [l], M. Simon [l]

[a] *INFN, Structure of Rome "Tor Vergata" and Physics Department of University of Rome "Tor Vergata", Via della Ricerca Scientifica 1, I-00133 Rome, Italy*
[b] *Moscow Engineering and Physics Institute, Kashirskoe Shosse 31, RU-115409 Moscow, Russia*
[c] *IFAC, Via Madonna del Piano 10, I-50019 Sesto Fiorentino, Florence, Italy*
[d] *INFN, Structure of Florence and Physics Department of University of Florence, Via Sansone 1, I-50019 Sesto Fiorentino, Florence, Italy*
[e] *INFN, Structure of Bari and Physics Department of University of Bari, Via Amendola 173, I-70126 Bari, Italy*
[f] *INFN, Structure of Naples and Physics Department of University of Naples "Federico II", Via Cintia, I-80126 Naples, Italy*
[g] *Lebedev Physical Institute, Leninsky Prospekt 53, RU-119991 Moscow, Russia*
[h] *Ioffe Physical Technical Institute, Polytekhnicheskaya 26, RU-194021 St. Petersburg, Russia*
[i] *INFN, Structure of Trieste and Physics Department of University of Trieste, Via A. Valerio 2, I-34127 Trieste, Italy*
[j] *INFN, Laboratori Nazionali di Frascati, Via Enrico Fermi 40, I-00044 Frascati, Italy*
[k] *KTH, Department of Physics, Albanova University Centre, SE-10691 Stockholm, Sweden*
[l] *Universität Siegen, D-57068 Siegen, Germany*

Received 9 November 2006; received in revised form 4 April 2007; accepted 17 July 2007

Abstract

PAMELA is a satellite borne experiment designed to study with great accuracy cosmic rays of galactic, solar, and trapped nature in a wide energy range (protons 80 MeV–700 GeV, electrons 50 MeV–400 GeV). Main objective is the study of the antimatter component: antiprotons (80 MeV–190 GeV), positrons (50 MeV–270 GeV) and search for antimatter with a precision of the order of 10^{-8}. The experiment, housed on board the Russian Resurs-DK1 satellite, was launched on June 15th, 2006 in a 350×600 km orbit with an inclination of 70°. The detector is composed of a series of scintillator counters arranged at the extremities of a permanent magnet spectrometer to provide charge, time-of-flight, and rigidity information. Lepton/hadron identification is performed by a silicon–tungsten calorimeter and a neutron detector placed at the bottom of the device. An anticounter system is used offline to reject false triggers coming from the satellite. In self-trigger mode the calorimeter, the neutron detector, and a shower tail catcher are capable of an

* Corresponding author. Tel.: +39 0672594575; fax: +39 0672594647.
E-mail address: Marco.Casolino@roma2.infn.it (M. Casolino).
† Deceased.

0273-1177/$34.00
doi:10.1016/j.asr.2007.07.023

independent measure of the lepton component up to 2 TeV. In this work we describe the experiment, its scientific objectives, and the performance in the first months after launch.

Keywords: Cosmic rays; Antimatter; Satellite borne experiment

1. Introduction

The Wizard collaboration is a scientific program devoted to the study of cosmic rays through balloon and satellite borne devices. Aims involve the precise determination of the antiproton (Boezio et al., 1997) and positron (Boezio et al., 2000) spectrum, search of antimatter, measurement of low energy trapped, and solar cosmic rays with the NINA-1 (Bidoli et al., 2001) and NINA-2 (Bidoli et al., 2003) satellite experiments. Other research on board Mir and International Space Station has involved the measurement of the radiation environment, the nuclear abundances, and the investigation of the Light Flash (Casolino et al., 2003) phenomenon with the Sileye experiments (Bidoli et al., 2001; Casolino, 2006c). PAMELA is the largest and most complex device built insofar by the collaboration, with the broadest scientific goals. In this work we describe the scientific objectives, the detector and the first in-flight performance of PAMELA.

2. Scientific objectives

PAMELA aims to measure in great detail the cosmic ray component at 1 AU (Astronomical Unit). Its 70°, 350×600 km orbit makes it particularly suited to study items of galactic, heliospheric, and trapped nature. Indeed for its versatility and detector redundancy PAMELA is capable to address at the same time a number of different cosmic ray issues ranging over a very wide energy range, from the trapped particles in the Van Allen Belts, to electrons of Jovian origin, to the study of the antimatter component. Here, we briefly describe the main scientific objectives of the experiment.

2.1. Antimatter research

The study of the antiparticle component ($\overline{p}$, e^+) of cosmic rays is the main scientific goal of PAMELA. A long term and detailed study of the antiparticle spectrum over a very wide energy spectrum will allow to shed light over several questions of cosmic ray physics, from particle production and propagation in the galaxy to charge dependent modulation in the heliosphere to dark matter detection. In Figs. 1 and 2 is shown the current status of the antiproton and positron measurements compared with PAMELA expected measurements in 3 years. In each case the two curves refer to a secondary only hypothesis with an additional contribution of a neutralino annihilation. Also cosmological issues related to detection of a dark matter signature and search for antimatter (PAMELA will search for $\overline{He}$ with a sensitivity of $\approx 10^{-8}$) will therefore be addressed with this device.

2.1.1. Antiprotons

PAMELA detectable energy spectrum of $\overline{p}$ ranges from 80 MeV to 190 GeV. Although the quality of $\overline{p}$ data has been improving in the recent years, a measurement of the energy spectrum of $\overline{p}$ will allow to greatly reduce the systematic error between the different balloon measurements, to study the phenomenon of charge dependent solar modulation, and will for the first time explore the energy range beyond $\simeq$40 GeV. Possible excesses over the expected secondary spectrum could be attributed to neutralino annihilation. In Profumo and Ullio (2004), Ullio (1999), and Donato et al. (2004) it is shown that PAMELA is capable of detecting an excess of antiprotons due to neutralino annihilation in models compatible with the WMAP measurements. Also Lionetto et al. (2005) estimate that PAMELA will be able to detect a supersymmetric signal in many minimal supergravity (mSUGRA) models. The possibility to extract a neutralino annihilation signal from the background depends on the parameters used, the boost factor (BF) and the galactic proton spectrum.

Charge dependent solar modulation, observed with the BESS balloon flights at Sun field reversal (Asaoka et al., 2002) will be monitored during the period of recovery going from the 23rd solar minimum going to the 24th solar maximum. Also the existence, intensity, and stability of secondary antiproton belts (Miyasaka et al., 2003), produced by the interaction of cosmic rays with the atmosphere will be measured.

2.1.2. Positrons

A precise measurement of the positron energy spectrum is needed to distinguish dark matter annihilation from other galactic sources such as hadronic production in giant molecular clouds, e^+/e^- production in nearby pulsars or decay from radioactive nuclei produced in supernova explosions. PAMELA is capable to detect e^+ in the energy range 50 MeV to 270 GeV. Possibilities for dark matter detection in the positron channel depend strongly on the nature of dark matter, its cross section, and the local inhomogeneity of the distribution. Hooper and Silk (2005) perform different estimation of PAMELA sensitivity according to different hypothesis of the dark matter component: detection is possible in case of an higgsino of mass up to 220 GeV (with $BF = 1$) and to 380 GeV (with $BF = 5$). Kaluza–Klein models (Hooper

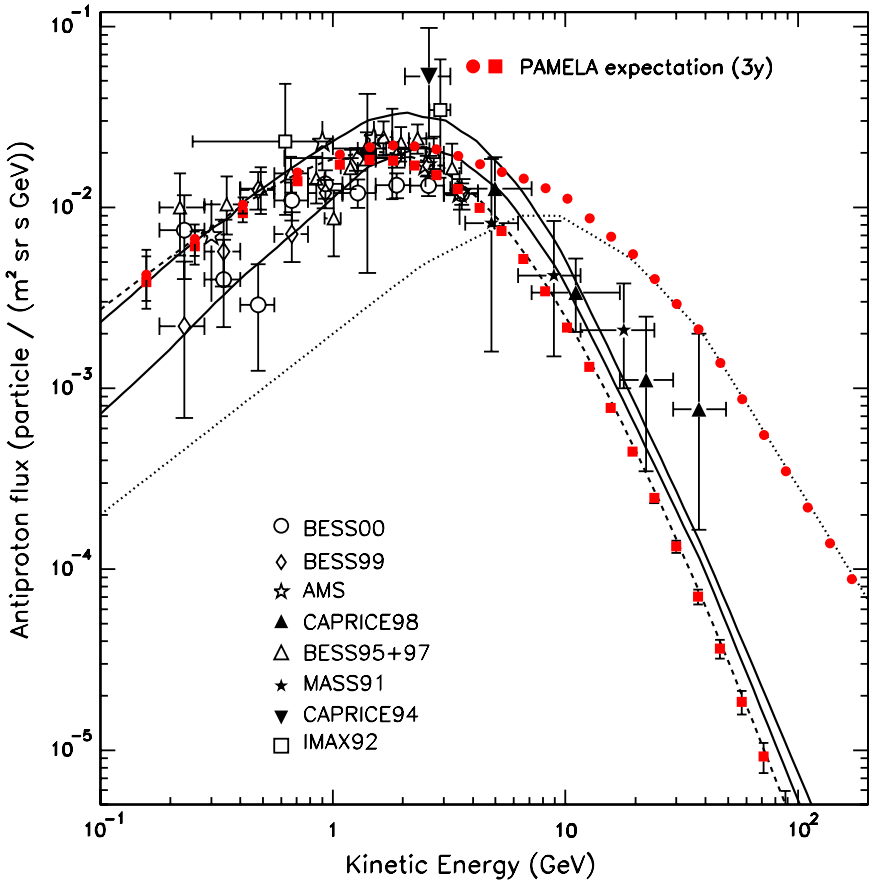

Fig. 1. Recent experimental $\bar{p}$ spectra (BESS00 and BESS99 (Asaoka et al., 2002), AMS (Aguilar et al., 2002), CAPRICE98 (Boezio et al., 2001), BESS95+97 (Orito et al., 2000), MASS91 (Hof et al., 1996), CAPRICE94 (Boezio et al., 1997), and IMAX92 (Mitchell et al., 1996)) along with theoretical calculations for pure $\bar{p}$ secondary production (solid lines: Simon et al. (1998), dashed line: Bergström (1999)) and for pure $\bar{p}$ primary production (dotted line: Ullio (1999), assuming the annihilation of neutralinos of mass 964 GeV/c^2).

and Kribs, 2004) would give a positron flux above secondary production increasing above 20 GeV and thus clearly compatible with PAMELA observational parameters. In case of a bino-like particle, as supposed by Minimal Supersymmetric Standard Model, PAMELA is sensible to cross sections of the order of $2\text{–}3 \times 10^{-26}$ (again, depending of BF). In case of Kaluza–Klein excitations of the Standard Model the sensitivity of PAMELA is for particles up to 350 and 550 GeV. In the hypothesis of the littlest Higgs model with T parity, the dark matter candidate is a heavy photon which annihilates mainly into weak gauge bosons in turn producing positrons. In Asano et al. (2006) it is shown that PAMELA will be able to identify this signal if the mass of the particle is below 120 GeV and the BF is 5. Hisano et al. (2006) assume a heavy wino-like dark matter component, detectable with PAMELA in the positron spectrum (and with much more difficulty in the antiproton channel) for mass of the wino above 300 GeV. This model predicts that if the neutralino has a mass of 2 TeV the positron flux increases by several orders of magnitude due to resonance of the annihilation cross section in W^+W^- and ZZ: in this scenario not only such a signal would be visible by PAMELA but also be consistent with the increase of positrons measured by HEAT (Barwick et al., 1991; Coutu et al., 1999). In conclusion a detailed measurement of the positron spectrum, its spectral features and its dependence from solar modulation will either provide evidence for a dark matter signature or strongly constrain and discard many existing models.

2.2. Galactic cosmic rays

Proton and electron spectra will be measured in detail with PAMELA. Also light nuclei (up to O) are detectable with the scintillator system. In this way it is possible to study with high statistics the secondary/primary cosmic ray nuclear and isotopic abundances such as B/C, Be/C, Li/C, and ^{3}He/^{4}He. These measurements will constrain existing production and propagation models in the galaxy, providing detailed information on the galactic structure and the various mechanisms involved.

2.3. Solar modulation of GCR

Launch of PAMELA occurred in the recovery phase of solar minimum toward cycle solar maximum of cycle 24. In this period it will be possible to observe solar modulation

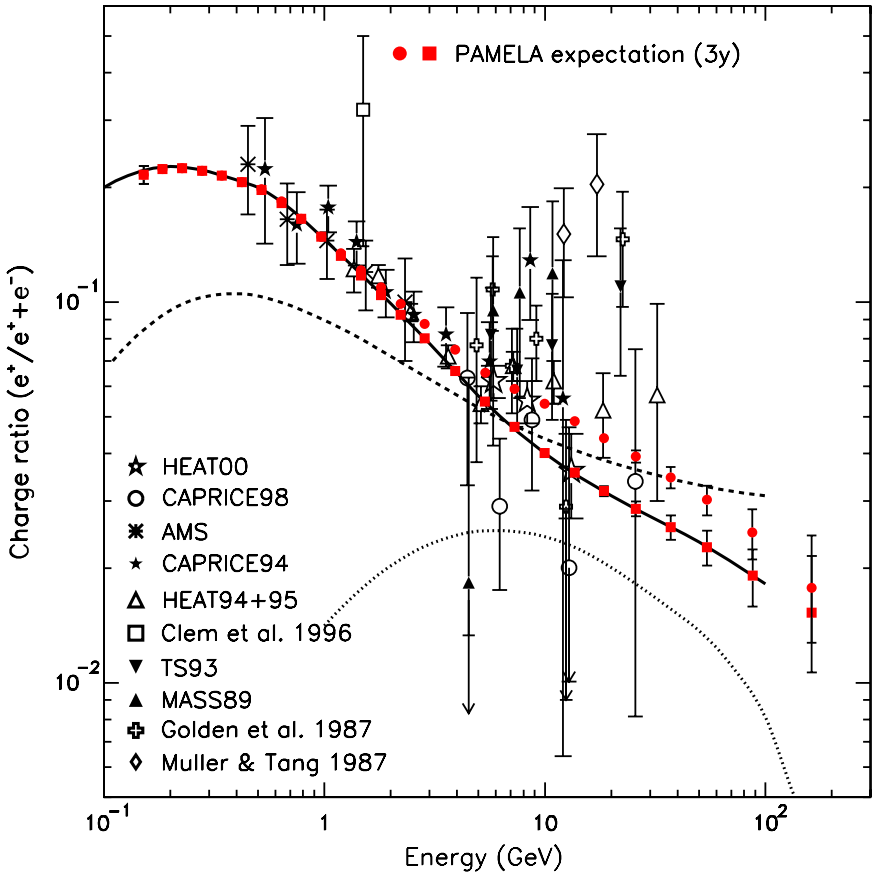

Fig. 2. The positron fraction as a function of energy measured by several experiments [(Golden et al., 1987; Müller and Tang, 1987; Clem et al., 1996) and MASS89 (Golden et al., 1994), TS93 (Golden et al., 1996), HEAT94+95 (Barwick et al., 1998), CAPRICE94 (Boezio et al., 2000; Barbiellini et al., 1996), AMS (Alcaraz et al., 2000), CAPRICE98 (Boezio et al., 2001), and HEAT00 (Beatty et al., 2004)]. The dashed (Protheroe, 1982) and the solid (Moskalenko and Strong, 1998) lines are calculations of the secondary positron fraction. The dotted line is a possible contribution from annihilation of neutralinos of mass 336 GeV/c^2 (Baltz and Edsjö, 1998). The expected PAMELA performance, in case of a pure secondary component (full boxes) and of an additional primary component (full circles), are indicated in both panels. Only statistical errors are included in the expected PAMELA data.

of galactic cosmic rays due to increasing solar activity. A long term measurement of the proton, electron, and nuclear flux at 1 AU will provide information on propagation phenomena occurring in the heliosphere. As already mentioned, the possibility to identify the antiparticle spectra will allow to study also charge dependent solar modulation effects.

2.4. Trapped particles

The 70° orbit of the Resurs-DK1 satellite allows for continuous monitoring of the electron and proton belts. The high energy (>80 MeV) component of the proton belt, crossed in the South Atlantic region will be monitored in detail with the magnetic spectrometer. Using the scintillator counting rates it will be possible to extend measurements of the particle spectra to lower energies using the range method. Monte Carlo simulations have shown that the coincidence of the two layers of the topmost scintillator (S1) allows PAMELA to detect e^- from 3.5 MeV and p from 36 MeV. Coincidence between S1 and the central scintillator (S2) allows us to measure integral spectra of 9.5 e^- and 63 MeV p. In this way it will be possible to perform a detailed mapping of the Van Allen Belts showing spectral and geometrical features. Also the neutron component will be measured, although some care needs to be taken to estimate the background coming from proton interaction with the main body of the satellite.

2.5. Solar energetic particles

We expect about 10 significant solar events during the experiment's lifetime with energy high enough to be detectable (Shea and Smart, 2001). The rate of background particles hitting the top trigger scintillator (S1) could be very high for intense solar events, hence a different trigger configuration has to be set in these cases. The usual trigger involves a coincidence of S1 with those located before (S2) and after (S3) the tracker. During solar particle events a devoted trigger mask (e.g., using only S2 and S3) can be programmed from ground.[1] The observation of solar ener-

[1] This can occur using information coming from the satellite monitoring system (e.g., SOHO, ACE, and GOES). In this way observation and memory filling would therefore vary according to the event type (impulsive, gradual) and intensity.

getic particle (SEP) events with a magnetic spectrometer will allow several aspects of solar and heliospheric cosmic ray physics to be addressed for the first time.

2.5.1. Electrons and positrons

Positrons are produced mainly in the decay of π^+ coming from nuclear reactions occurring at the flare site. Up to now, they have only been measured indirectly by remote sensing of the gamma ray annihilation line at 511 keV. Using the magnetic spectrometer of PAMELA it will be possible to separately analyze the high energy tail of the electron and positron spectra at 1 AU obtaining information both on particle production and charge dependent propagation in the heliosphere in perturbed conditions of solar particle events.

2.5.2. Protons

PAMELA will be able to measure the spectrum of cosmic ray protons from 80 MeV up to almost 1 TeV and therefore will be able to measure the solar component over a very wide energy range (where the upper limit will be limited by statistics). These measurements will be correlated with other instruments placed in different points of the Earth's magnetosphere to give information on the acceleration and propagation mechanisms of SEP events. Up to now there has been no direct measurement (Miroshnichenko, 2001) of the high energy (>1 GeV) proton component of SEPs. The importance of a direct measurement of this spectrum is related to the fact (Ryan, 2000) that there are many solar events where the energy of protons is above the highest ($\simeq$100 MeV) detectable energy range of current spacecrafts, but is below the detection threshold of ground Neutron Monitors (Bazilevskaya and Svirzhevskaya, 1998). However, over the PAMELA energy range, it will be possible to examine the turnover of the spectrum, where we find the limit of acceleration processes at the Sun. The instrument has a maximum trigger rate of about 60 Hz and a geometrical factor of 21.5 cm^2 sr. This implies that we will be able to read all events with an integral flux (above 80 MeV) up to 4 particles/cm^2 s sr. For such events we expect about 2×10^6 particles/day (assuming a spectral index of $\gamma = 3$ we have 2×10^3 events/day above 1 GeV).

2.5.3. Nuclei

PAMELA can identify light nuclei up to Carbon and isotopes of Hydrogen and Helium. Thus, we can investigate the light nuclear component related to SEP events over a wide energy range. This should contribute to establish whether there are differences in the composition of the high energy (1 GeV) ions to the low energy component ($\simeq$20 MeV) producing γ rays or the quiescent solar corona (Ryan, 2005).

Applying the same estimates as above, we can expect $\simeq 10^4$ ^{4}He and $\simeq 10^2$ ^{3}He nuclei for gradual events, and more for impulsive (often ^{3}He enriched) ones. Such a high statistics will allow us to examine in detail the amount of the ^{3}He and deuterium (up to 3 GeV/c). These measurements will help us to better understand the selective acceleration processes in the higher energy impulsive (Reames, 1999) events.

2.5.4. Neutrons

Neutrons are produced in nuclear reactions at the flare site and can reach the Earth before decaying (Chupp et al., 1982). Although there is no devoted trigger for neutrons in PAMELA, the background counting of the neutron detector will measure in great detail the temporal profile and distribution of solar neutrons. The background counting system keeps track of the number of neutrons which hit the neutron detector in the time elapsed since last trigger. The counter is reset each time it is read allowing for a precise measurement of background neutron conditions during the mission. On the occurrence of solar events, neutrons are expected to reach Earth before protons as they have no charge. They are not deflected by any magnetic field and will be directly recorded by PAMELA (if it is not in Earth's shadow).

2.5.5. Lowering of the geomagnetic cutoff

The high inclination of the orbit of the Resurs-DK1 satellite will allow PAMELA to study (Ogliore et al., 2001; Leske et al., 2001) the variations of cosmic ray geomagnetic cutoff due to the interaction of the SEP events with the geomagnetic field.

2.6. Jovian electrons

Since the discovery made by the Pioneer 10 satellite of Jovian electrons at about 1 AU from Jupiter (Simpson et al., 1974; Eraker, 1982), with an energy between 1 and 25 MeV, several interplanetary missions have measured this component of cosmic rays. Currently we know that Jupiter is the strongest electron source at low energies (below 25 MeV) in the heliosphere within a radius of 11 AUs. Its spectrum has a power law with spectral index $\gamma = 1.65$, increasing above 25 MeV, where the galactic component becomes dominant. At 1 AU from the Sun the IMP-8 satellite could detect Jovian electrons in the range between 0.6 and 16 MeV and measure their modulation by the passage of Coronal Interaction Regions (CIR) with 27 days periodicity (Eraker, 1982; Chenette, 1980). There are also long term modulation effects related to the Earth–Jupiter synodic year of 13 months duration. In fact, since Jovian electrons follow the interplanetary magnetic field lines, when the two planets are on the same solar wind spiral line, the electron transit from Jupiter to the Earth is eased and the flux increases. On the other side, when the two planets lie on different spiral lines the electron flux decreases. For PAMELA the minimum threshold energy for electron detection is 50 MeV. In this energy range, however, geomagnetic shielding will reduce the active observation time reducing total counts. Nevertheless it will be

possible to study for the first time the high energy Jovian electron component and test the hypothesis of reacceleration at the solar wind Termination Shock (TS). It is known that cosmic rays originating outside the heliosphere can be accelerated at the solar wind TS. This applies also to Jovian electrons, which are transported outward by the solar wind, reach the TS and undergo shock acceleration thus increasing their energy. Some of these electrons are scattered back in the heliosphere. The position of the shock (still unknown and placed at about 80–100 AU) can affect the reaccelerated electron spectrum (Potgieter and Ferreira, 2002; Fichtner et al., 2001). Overall, Jovian electrons are dominant in the energy range 50–70 MeV and decrease in intensity to about 1% of the total galactic flux above 70 MeV. This component can however be extracted from the galactic background with observation periods of the order of 4–5 months (Casolino, 2006a). In addition it is possible that the reacceleration of electrons at the solar wind TS is modulated by the solar cycle; 3 years of observations in the recovering phase of the solar minimum should show such effects.

2.7. High energy lepton component

The calorimeter can provide an independent trigger to PAMELA for high energy releases due to showers occurring in it: a signal is generated with the release of energy above 150 mip in all the 24 views of planes from 7 to 18. With this requirement the geometrical factor of the calorimeter self-trigger is 400 cm^2 sr if events coming from the satellite are rejected. In this way it is possible to study the electron and positron flux in the energy range between 300 GeV and 2 TeV, where measurements are currently scarce (Kobayashi, 1999). At this energy discrimination with hadrons is performed with topological and energetic discrimination of the shower development in the calorimeter coupled with neutron information coming from the neutron detector. This is because neutron production cross section in an e.m. cascade is lower than in a hadronic cascade (Galper, 2001).

3. Instrument description

In this section we describe the main characteristics of PAMELA detector; a more detailed description of the device and the data handling can be found in Picozza et al. (2007), Casolino (2006b), and Casolino et al. (2006). The device (Fig. 3) is constituted by a number of highly redundant detectors capable of identifying particles providing charge, mass, rigidity, and beta over a very wide energy range. The instrument is built around a permanent magnet with a silicon microstrip tracker with a scintillator system to provide trigger, charge, and time-of-flight information. A silicon–tungsten calorimeter is used to perform hadron/lepton separation. A shower tail catcher and a neutron detector at the bottom of the apparatus increase this separation. An anticounter system is used to reject spurious events in the off-line phase. Around the detectors are housed the readout electronics, the interfaces with the

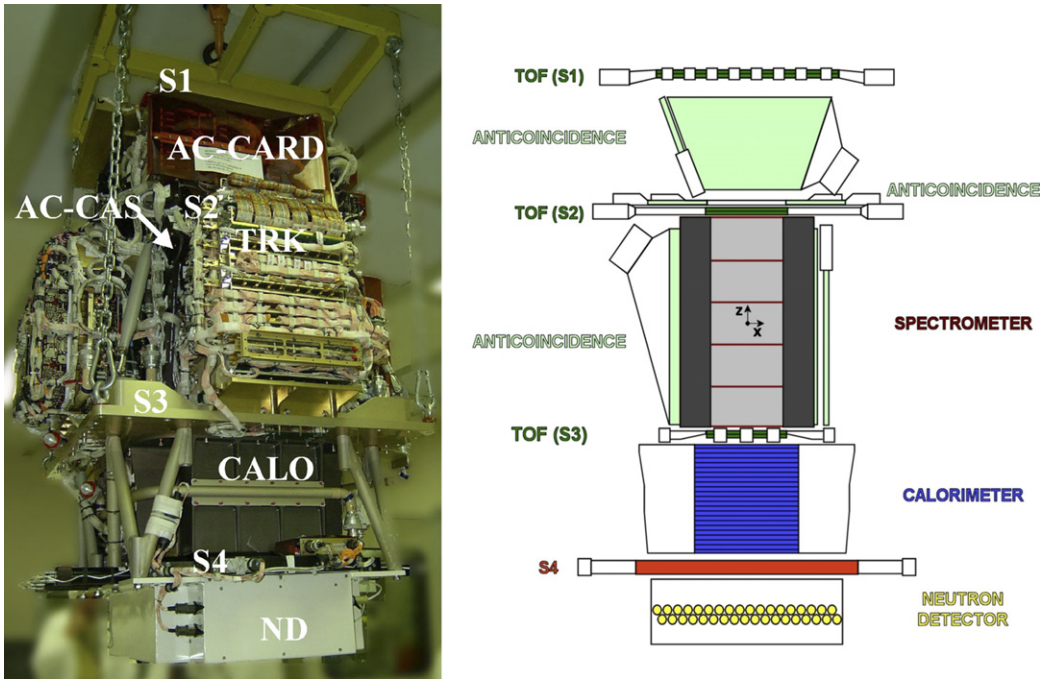

Fig. 3. Left: photo of the PAMELA detector during the final integration phase in Tor Vergata clean room facilities, Rome. It is possible to discern, from top to bottom, the topmost scintillator system, S1, the electronic crates around the magnet spectrometer, the baseplate (to which PAMELA is suspended by chains), the black structure housing the Si–W calorimeter, S4 tail scintillator and the neutron detector. Right: scheme – approximately to scale with the picture – of the detectors composing PAMELA.

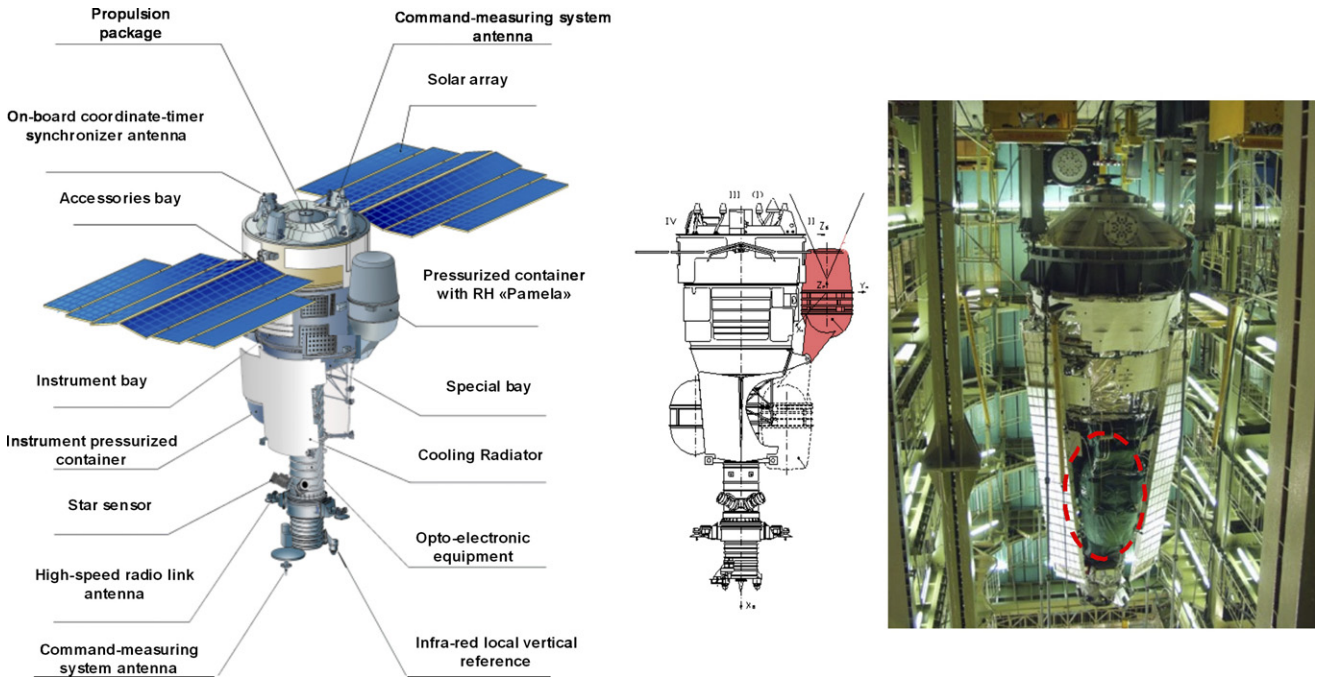

Fig. 4. Left: scheme of the Resurs-DK1 satellite. PAMELA is located in the pressurized container on the right of the picture. In the center panel it is possible to see the container in the launch position and in the extended (cosmic ray acquisition) configuration. In the right panel it is possible to see a picture of the satellite in the assembly facility in Samara. The picture is rotated 180° to compare the photo with the scheme. The dashed circle shows the location of PAMELA pressurized container in the launch position.

CPU and all primary and secondary power supplies. All systems (power supply, readout boards, etc.) are redundant with the exception of the CPU which is more tolerant to failures. The system is enclosed in a pressurized container (Figs. 4 and 5) located on one side of the Resurs-DK satellite. In a twin pressurized container is housed the Arina experiment, devoted to the study of the low energy trapped electron and proton component. Total weight of PAMELA is 470 kg; power consumption is 355 W, geometrical factor is 21.5 cm^2 sr.

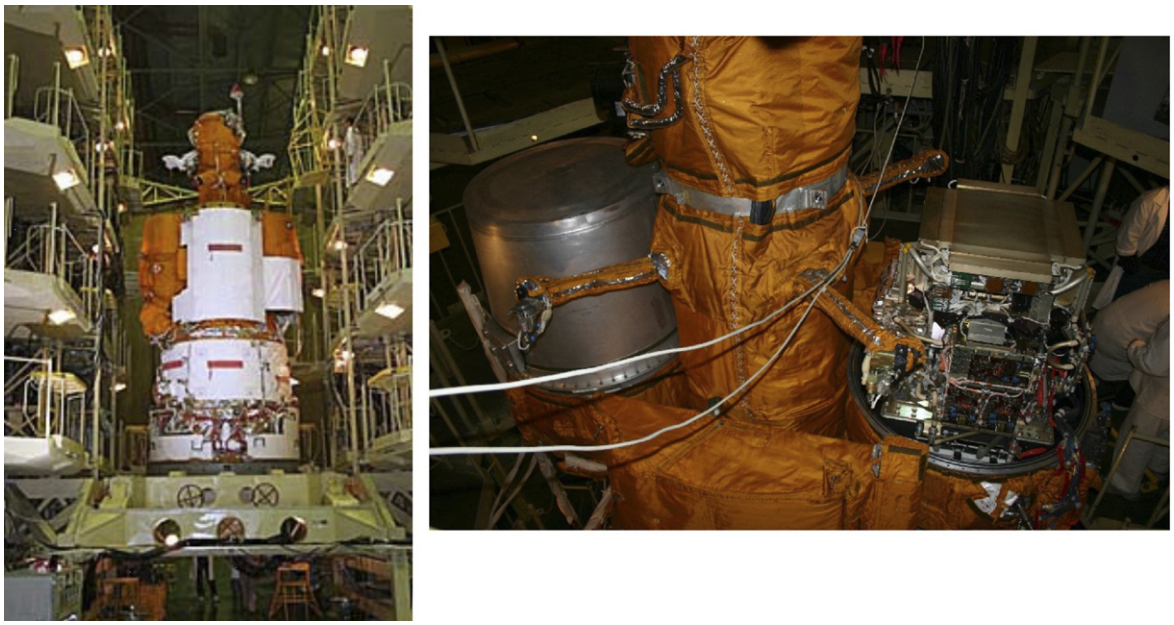

Fig. 5. Left: photo of Resurs in the final integration phase in Baikonur. It is possible to discern the optical sensor on top, the two pressurized containers on the sides, and the white heat cooling panel in the forefront. Right: close up picture of the integration phase of PAMELA in the pressurized container (right in picture).

3.1. Scintillator/time-of-flight

The scintillator system (Barbarino et al., 2003) provides trigger for the particles and time-of-flight information for incoming particles. There are three scintillators layers, each composed by two orthogonal planes divided in various bars (8 for S11, 6 for S12, 2 for S21 and S22, and 3 for S32 and S33) for a total of 6 planes and 48 phototubes (each bar is read by two phototubes). S1 and S3 bars are 7 mm thick and S2 bars are 5 mm. Interplanar distance between S1 and S3 of 77.3 cm results in a TOF determination of 250 ps precision for protons and 70 ps for C nuclei (determined with beam tests in GSI), allowing separation of electrons from antiprotons up to $\simeq$1 GeV and albedo rejection. The scintillator system is also capable of providing charge information up to $Z = 8$.

3.2. Magnetic spectrometer

The permanent magnet (Adriani et al., 2003) is composed of 5 blocks, each divided in 12 segments of Nd–Fe–B alloy with a residual magnetization of 1.3 T arranged to provide an almost uniform magnetic field along the y direction. The size of the cavity is $13.1 \times 16.1 \times 44.5\ \mathrm{cm}^3$, with a mean magnetic field of 0.43 T. Six layers of 300 μm thick double-sided microstrip silicon detectors are used to measure particle deflection with 3.0 ± 0.1 and 11.5 ± 0.6 μm precision in the bending and non-bending views. Each layer is made by three ladders, each composed by two $5.33 \times 7.00\ \mathrm{cm}^2$ sensors coupled to a VA1 front-end hybrid circuit. Maximum Detectable Rigidity (MDR) was measured on CERN proton beam to be $\simeq$1 TV.

3.3. Silicon–tungsten calorimeter

Lepton/hadron discrimination is performed by the silicon–tungsten sampling calorimeter (Boezio et al., 2002) located on the bottom of PAMELA. It is composed of 44 silicon layers interleaved by 22 0.26 cm thick tungsten plates. Each silicon layer is composed arranging 3×3 wafers, each of $80 \times 80 \times .380\ \mathrm{mm}^3$ and segmented in 32 strips, for a total of 96 strips/plane. Twenty-two planes are used for the X view and 22 for the Y view in order to provide topological and energetic information of the shower development in the calorimeter. Tungsten was chosen in order to maximize electromagnetic radiation lengths ($16.3X_0$) minimizing hadronic interaction length (0.6λ). The CR1.4P ASIC chip is used for front-end electronics, providing a dynamic range of 1400 mips (minimum ionizing particles) and allowing nuclear identification up to Iron.

3.4. Shower tail scintillator

This scintillator ($1 \times 48 \times 48\ \mathrm{cm}^3$) is located below the calorimeter and is used to improve hadron/lepton discrimination by measuring the energy not contained in the shower of the calorimeter. It can also function as a stand-alone trigger for the neutron detector.

3.5. Neutron detector

The $60 \times 55 \times 15\ \mathrm{cm}^3$ neutron detector is composed by 36 ^{3}He tubes arranged in two layers and surrounded by polyethylene shielding and a 'U' shaped cadmium layer to remove thermal neutrons not coming from the calorimeter. It is used to improve lepton/hadron identification by detecting the number of neutrons produced in the hadronic and electromagnetic cascades. Since the former have a much higher neutron cross section than the latter, where neutron production comes essentially through nuclear photofission, it is estimated that PAMELA overall identifi-

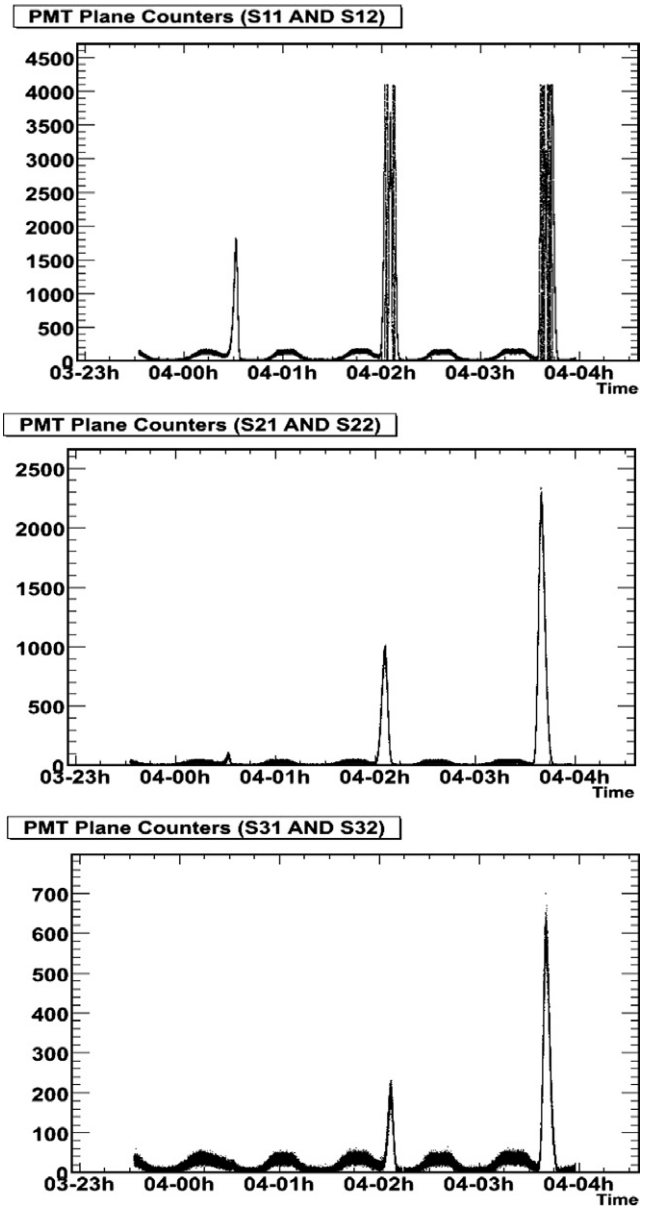

Fig. 6. Counting rates of PAMELA (ADC channels) as a function of time.

cation capability is improved by a factor 10. As already mentioned, the neutron detector is used to measure neutron field in Low Earth Orbit and in case of solar particle events as well as in the high energy lepton measurement.

3.6. Anticoincidence system

To reject spurious triggers due to interaction with the main body of the satellite, PAMELA is shielded by a number of scintillators used with anticoincidence functions (Orsi et al., 2006; Pearce, 2003). CARD anticoincidence system is composed of four 8 mm thick scintillators located in the area between S1 and S2. CAT scintillator is placed on top of the magnet: it is composed by a single piece with a central hole where the magnet cavity is located and read out by 8 phototubes. Four scintillators, arranged on the sides of the magnet, make the CAS lateral anticoincidence system.

4. Integration and launch

PAMELA was integrated in INFN – Tor Vergata clean room facilities, Rome; tests involved first each subsystem separately and subsequently the whole apparatus simulating all interactions with the satellite using an Electronic Ground Support Equipment. Final tests involved cosmic ray acquisitions with muons for a total of about 480 h. The device was then shipped to Tskb Progress plant, in Samara (Russia), for installation in a pressurized container on board the Resurs-DK satellite for final tests. Also in this case acquisitions with cosmic muons (140 h) have been performed and have shown the correct functioning of the apparatus, which was then integrated with the pressurized container and the satellite. In 2006 the final integration phase took place in Baikonur cosmodrome in Kazakstan.

Launch occurred with Soyuz-U rocket on June 15th, 2006, 08:00:00.193 UTC, orbital insertion was in a parking orbit of semimajor axis of 6642 km. Final boost occurred on June 18th, 2006 when the orbit was raised to a semimajor axis of 6828 km.

Altitude of the satellite is usually minimum in the northern hemisphere and maximum in the southern hemisphere since its primary goal is to perform earth observations and resolution of the pictures increases at lower altitudes. To compensate for atmospheric drag, the altitude of the satellite is periodically reboosted by vernier engines. To perform this manoeuvre the pressurized container housing PAMELA is folded back in the launch position, the satellite is rotated 180° on its longitudinal axis and then engines are started. Reboost frequency depends from orbital decay, due to atmospheric drag, in turn caused by solar activity. Up to October 2006 the activity has been low with only two small solar particle events, so there has not been the need to perform this maneuver yet. Resurs-DK1 oscillates on its longitudinal axis when performing Earth observations: a detailed information of the attitude of the satellite is provided to the CPU of PAMELA in order to know the orientation of the detector with precision of $\simeq 1°$.

5. In-flight data

PAMELA was first switched on June 26th, 2006. A typical behaviour of the acquisition of the device is shown in Fig. 6. The three panels show the counting rate of the three planes and correspond to particles of increasing energy: S11*S12 is triggered by 36 MeV protons and 3.5 MeV e^-, S21*S22 requires protons and electrons of 9.5 and 63 MeV, respectively, and S31*S32 requires protons and electrons of 80 and 50 MeV (lower energy particles may penetrate the detector from the sides and increase the trigger rate). The higher energy cut is evident in the counting rate of the scintillators: the first SAA passage, corresponding to the easternmost

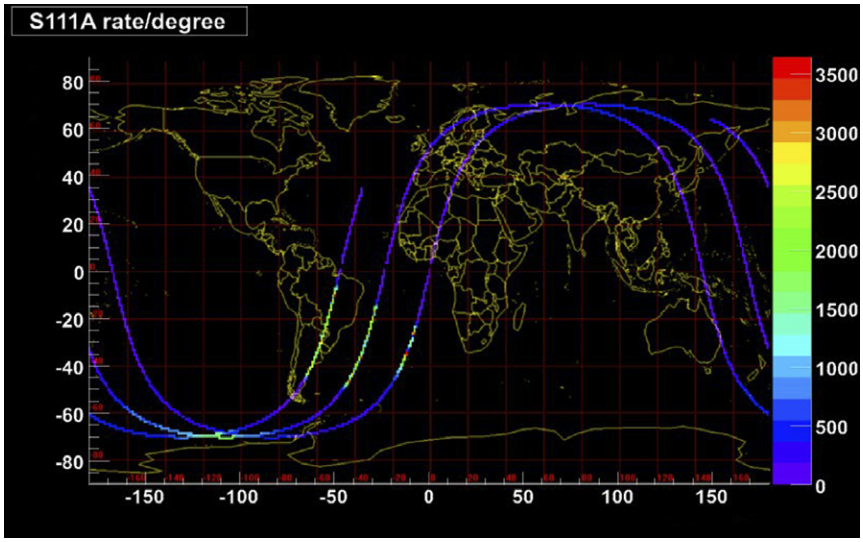

Fig. 7. Ground track of PAMELA with counting rate of S11*S12 trigger. Note the particle rate increase in the South Atlantic Anomaly.

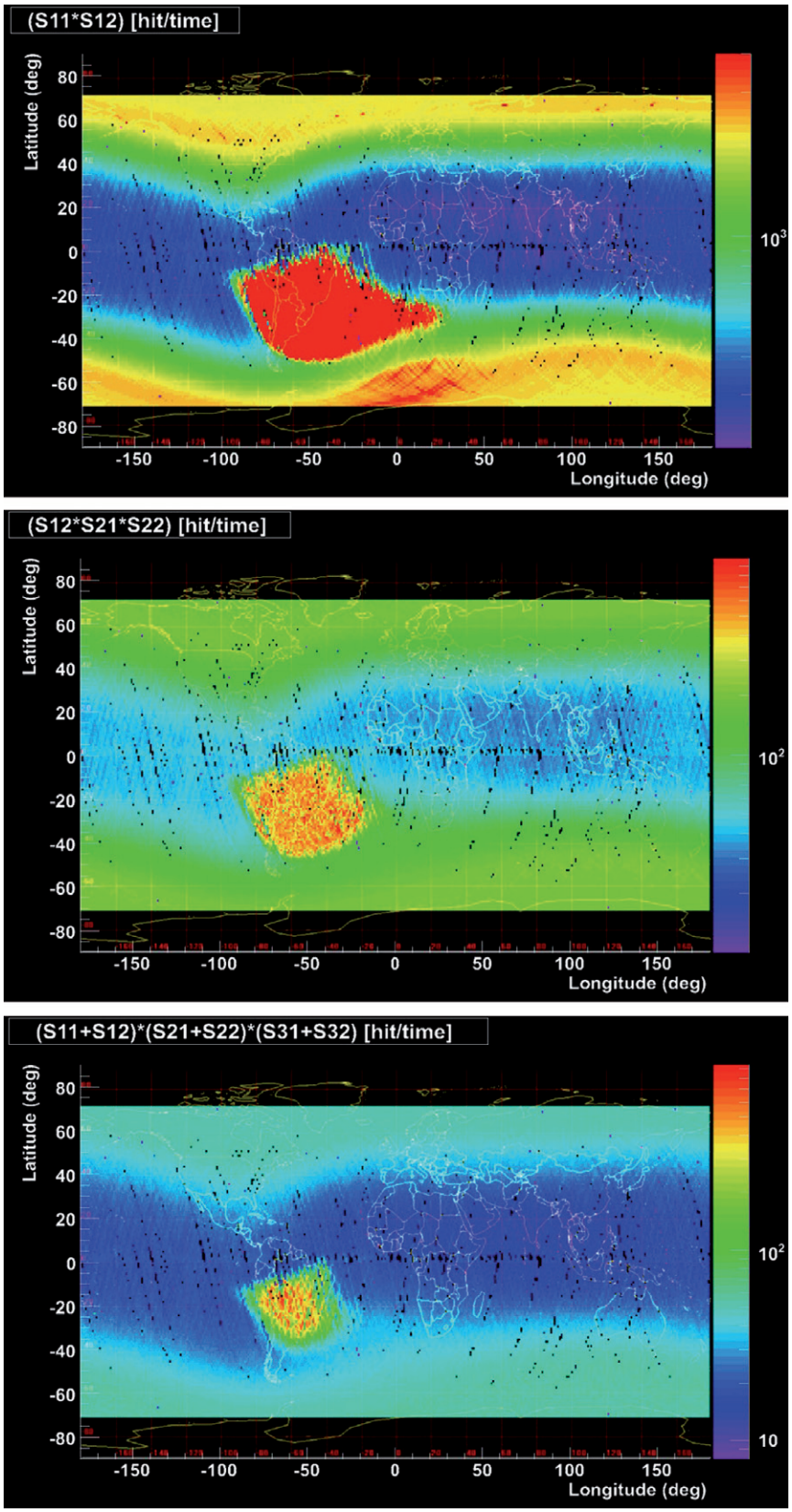

Fig. 8. Counting rates of various trigger counters of the scintillators. Top panel: S11*S12 (p 36 MeV, e^- 3.5 MeV). Center panel: S12*S21*S22 (p 63 MeV, e^- 9.5 MeV). Bottom panel: (S11 + S12)*(S21 + S22)*(S31 + S32) (p 80 MeV, e^- 50 MeV).

passage, is absent in the S3 counting rate. The other two passages in the SAA saturate several times the ADC counting rate of the S1 scintillator but not the other two scintillators. This is consistent with the power law

spectrum of trapped particles in the SAA and the geometrical ratio between the two scintillators. Also S2 and S3 counting rate ratio in the anomaly is about 5, consistent with a particle flux ratio evaluated with AP8 algorithm (Gaffey, 1994). Outside the SAA it is possible to see the increase of particle rate at the geomagnetic poles due to the lower geomagnetic cutoff. The highest rates are found when the satellite crosses the trapped components of the Van Allen Belts. Fig. 7 shows the same trigger rate as a function of the ground track of PAMELA. It is possible to see the inclination of the orbit of satellite and the particle rate increase in the polar and South Atlantic regions. The pause in the acquisition at the equator are due to the calibration of the subdetectors usually performed during the ascending phase to avoid crossing the radiation belts. In Fig. 8 is shown PAMELA world particle rate for S1*S2 counter, exhibiting the high latitude electron radiation belts and the proton belt in the South Atlantic Anomaly. Note that the northern electron belt is less intense than the southern one because PAMELA orbit is $\simeq$350 km in that region as compared to the $\simeq$600 km in the south. In the same figure, panel 2 is shown the same map for S12*S21*S22 trigger configuration, corresponding to 9.5 MeV electrons and 63 MeV protons. In this case the intensity of the electron belts is reduced and size of the SAA is smaller, as expected for higher energy protons.

6. Conclusions

PAMELA was successfully launched on June 2006 and is currently operational in Low Earth Orbit. The satellite and the detectors are functioning correctly. It is expected that data from PAMELA will provide information on several items of cosmic ray physics, from antimatter to solar and trapped particles.

References

Adriani, O., Bonechi, L., Bongi, M., et al. The magnetic spectrometer of the PAMELA satellite experiment. Nucl. Instr. Meth. Phys. Res. A 511, 72, 2003.

Aguilar, M., Alcaraz, J., Allaby, J., Alpat, B., Ambrosi, G., Anderhub, H., Ao, L., Arefiev, A., Azzarello, P., Babucci, E., et al. The Alpha Magnetic Spectrometer (AMS) on the International Space Station: Part I results from the test flight on the space shuttle. Phys. Rep. 366, 331–405, 2002.

Alcaraz, J., Alpat, B., Ambrosi, G., Anderhub, H., Ao, L., Arefiev, A., Azzarello, P., Babucci, E., et al. Leptons in near earth orbit. Phys. Lett. B 484, 10–22, 2000.

Asano, M., Matsumoto, S., Okada, N., Okada, Y. Cosmic positron signature from dark matter in the littlest Higgs model with T-parity. Available from: <hep-ph/0602157v1>, 17 Feb 2006.

Asaoka, Y., Shikaze, Y., Abe, K., et al. Measurements of cosmic-ray low-energy antiproton and proton spectra in a transient period of solar field reversal. Phys. Rev. Lett. 88, 051101. Available from:, 2002 <astro-ph/0109007>, 2001, 2006.

Baltz, E.A., Edsjö, J. Positron propagation and fluxes from neutralino annihilation in the halo. Phys. Rev. D 59, 023511, 1998.

Barbarino, G.C., Boscherini, M., Campana, D., Filrnkranz, W., Menn, W., Orazi, M., Osteria, G., et al. The PAMELA time-of-flight system: status report. Nucl. Phys. (Proc. Suppl.) B 125, 298, 2003.

Barwick, S.W., Beatty, J.J., Bower, C.R., et al. The energy spectra and relative abundances of electrons and positrons in the galactic cosmic radiation. Astrophys. J. 498, 779, 1998.

Barwick, S.W., Beatty, J.J., Bhattacharyya, A., et al. Measurements of the cosmic-ray positron fraction from 1 to 50 GeV. Astrophys. J. 482, L191, 1991.

Bazilevskaya, G.A., Svirzhevskaya, A.K. On the stratospheric measurements of cosmic rays. Space Sci. Rev. 85, 431, 1998.

Beatty, J.J., Bhattacharyya, A., Bower, C., et al. New measurement of the cosmic-ray positron fraction from 5 to 15 GeV. Phys. Rev. Lett. 93, 241102. Available from:, 2004 <astro-ph/0412230>, 2004, 1998.

Bergström, L., Ullio, P. Private communication, 1999.

Bidoli, V., Canestro, A., Casolino, M., et al. In orbit performance of the space telescope NINA and galactic cosmic-ray flux measurements. Astrophys. J. 132, 365, 2001.

Bidoli, V., Casolino, M., De Pascale, M., et al. Isotope composition of secondary hydrogen and helium above the atmosphere measured by the instruments NINA and NINA-2. J. Geophys. Res. 108 (A5), 1211, 2003.

Boezio, M., Barbiellini, G., Spinelli, P., et al. The cosmic ray antiproton flux between 0.62 and 3.19 GeV measured near solar minimum activity. Astrophys. J. 487, 415, 1997.

Boezio, M., Carlson, P., Francke, T. The cosmic-ray electron and positron spectra measured at 1 AU during solar minimum activity. Astrophys. J. 532, 653, 2000.

Barbiellini, G., Basini, G., Bellotti, R., et al. The cosmic-ray positron-to-electron ratio in the energy range 0.85 to 14 GeV. Astron. Astrophys. 309, L15, 1996.

Boezio, M., Bonvicini, V., Schiavon, P., et al. The cosmic-ray antiproton flux between 3 and 49 GeV. Astrophys. J. 561, 787. Available from:, 2001 <astro-ph/0103513>, 1996.

Boezio, M., Barbiellini, G., Bonvicini, V., et al. Measurements of cosmic-ray electrons and positrons by the Wizard/CAPRICE collaboration. Adv. Space Res. 27, 669, 2001.

Boezio, M., Bonvicini, V., Mocchiutti, E., et al. A high granularity imaging calorimeter for cosmic-ray physics. Nucl. Instr. Meth. Phys. Res. A 487, 407, 2002.

Bidoli, V., Casolino, M., De Grandis, E., et al. In-flight performance of SilEye-2 experiment and cosmic ray abundances inside the Mir space station. J. Phys. G 27, 2051, 2001.

Casolino, M., Bidoli, V., Morselli, A., et al. Dual origins of light flashes seen in space. Nature, 422, 2003.

Casolino, M. Cosmic ray observation of the heliosphere with the PAMELA experiment. Adv. Space Res. 37 (10), 1848–1852, 2006a.

Casolino, M. The PAMELA storage and control unit. Adv. Space Res. 37 (10), 1857, 2006b.

Casolino, M. Sileye-3/Alteino Collaboration, Detector response and calibration of the cosmic-ray detector of the Sileye-3/Alteino experiment. Adv. Space Res. 37 (9), 1691, 2006c.

Casolino, M., De Pascale, M.P., Nagni, M., Picozza, P. YODA++: a proposal for a semi-automatic space mission control. Adv. Space Res. 37 (10), 1884, 2006.

Coutu, S., Barwick, S.W., Beatty, J.J., et al. Cosmic-ray positrons: are there primary sources? Astropart. Phys. 11, 429, 1999.

Chenette, D.L. The propagation of Jovian electrons to earth. J. Geophys. Res. 85, 2243, 1980.

Chupp, E.L., Forrest, D.J., Ryan, J.M., et al. A direct observation of solar neutrons following the 0118 UT flare on 1980 June 21. Astrophys. J. 263, L95 , 1982.

Clem, J.M., Clements, D.P., Esposito, J., et al. Solar modulation of cosmic electrons. Astrophys. J. 464, 507, 1996.

Donato, F., Fornengo, N., Maurin, D., Salati, P., Taillet, R. Antiprotons in cosmic rays from neutralino annihilation. Phys. Rev. D 69, 63501, 2004.

Eraker, J.H. Origins of the low-energy relativistic interplanetary electrons. Astrophys. J. 257, 862, 1982.

Fichtner, H., Potgieter, M.S., Ferreira, S.E.S., Heber, B., Burger, R.A. Effects of the solar wind termination shock on the modulation of Jovian and galactic electrons in the heliosphere, in: Proceedings of the 27th Int. Cosmic Ray Conference, Hamburg, SH 3666, 2001.

Gaffey, J., Bilitza, D. NASA/National Space Science Data Center trapped radiation models, J. Spacecraft Rockets 31(2), 172, 1994. Available from: <http://modelweb.gsfc.nasa.gov/magnetos/aeap.html>.

Galper, A.M. for PAMELA collaboration. Measurement of primary protons and electrons in the energy range of 10^{11}–10^{13} eV in the PAMELA experiment, in: Proceedings of the 27th International Cosmic Ray Conference, Hamburg, OG 2219, 2001.

Golden, R.L., Mauger, B.G., Horan, S., Stephens, S.A., Daniel, R.R., Badhwar, G.D., Lacy, J.L., Zipse, J.E. Observation of cosmic ray positrons in the region from 5 to 50 GeV. Astron. Astrophys. 188, 145, 1987.

Golden, R.L., Grimani, C., Kimbell, B.L. Observations of cosmic-ray electrons and positrons using an imaging calorimeter. Astrophys. J. 436, 769, 1994.

Golden, R.L., Stochaj, S.J., Stephens, S.A., et al. Measurement of the positron to electron ratio in the cosmic rays above 5 GeV. Astrophys. J. 457, L103, 1996.

Hof, M., Menn, W., Pfeifer, C., et al. Measurement of cosmic ray antiprotons from 3.7 to 19 GeV. Astrophys. J. 467, L33, 1996.

Hooper, D., Silk, J. Searching for dark matter with future cosmic positron experiments. Phys. Rev. D 71, 083503, 2005.

Hooper, D., Kribs, G.D. Kaluza–Klein dark matter and the positron excess. Phys. Rev. D 70, 115004, 2004.

Hisano, J., Matsumoto, S., Saito, O., Senami, M. Heavy wino-like neutralino dark matter annihilation into antiparticles. Phys. Rev. D 73, 055004, 2006.

Kobayashi, T. High energy cosmic-ray electrons beyond 100 GeV, in: Proceedings of the 26th International Cosmic Ray Conference, vol. 3, pp. 61–64, 1999.

Leske, R.A., Mewaldt, R.A., Stone, E.C., von Rosenvinge, T.T. Observations of geomagnetic cutoff variations during solar energetic particle events and implications for the radiation environment at the Space Station. J. Geophys. Res. A 12, 30011, 2001.

Lionetto, A.M., Morselli, A., Zdravkovic, V. Uncertainties of cosmic ray spectra and detectability of antiproton mSUGRA contributions with PAMELA, JCAP 0509 010, 2005. Available from: <astro-ph/0502406>.

Miroshnichenko, L. Solar Cosmic Rays. Kluwer, 2001.

Mitchell, J.W., Barbier, L.M., Christian, E.R., et al. Measurement of 0.253.2 GeV antiprotons in the cosmic radiation. Phys. Rev. Lett. 76, 3057, 1996.

Miyasaka, H., Gusev, A., Pugacheva, G., Schuch, N.J., Jayanthi, U.B, Spjeldvik, W. Cosmic ray produced antiprotons confined in the innermost magnetosphere, in: Proceedings of the 28th International Cosmic Ray Conference, Tsukuba, Japan, 4265, 2003.

Moskalenko, I.V., Strong, A.W. Production and propagation of cosmic-ray positrons and electrons. Astrophys. J. 493, 694, 1998.

Müller, D., Tang, K. Cosmic-ray positrons from 10 to 20 GeV – a balloon-borne measurement using the geomagnetic east–west asymmetry. Astrophys. J. 312, 183, 1987.

Ogliore, R.C., Mewaldt, R.A., Leske, R.A., et al. A direct measurement of the geomagnetic cutoff for cosmic rays at space station latitudes, in: Proceedings of the 27th International Cosmic Ray Conference, Hamburg, 2001.

Orito, S., Maeno, T., Matsunaga, H., et al. Precision measurement of cosmic-ray antiproton spectrum. Phys. Rev. Lett. 84, 1078, 2000.

Orsi, S., Carlson, P., Lund, J., et al. The anticoincidence shield of the PAMELA space experiment. Adv. Space Res. 37 (10), 1853–1856, 2006.

Pearce, M. The anticounter system of the PAMELA space experiment, in: Proceedings of the 28th International Cosmic Ray Conference, Tsukuba, Japan, OG 1.5, 2125, 2003.

Potgieter, M.S., Ferreira, S.E.S. Effects of the solar wind termination shock on the modulation of Jovian and galactic electrons in the heliosphere. J. Geophys. Res. A 7, SSH 1, 2002.

Picozza, P., Galper, A.M., Castellini, G. PAMELA – a payload for antimatter matter exploration and light-nuclei astrophysics. Astropart. Phys. 27 (4), 296, 2007.

Profumo, S., Ullio, P. The role of antimatter searches in the hunt for supersymmetric dark matter. JCAPP, 07, 006, 2004.

Protheroe, R.J. On the nature of the cosmic ray positron spectrum. Astrophys. J. 254, 391, 1982.

Reames, D.V. Particle acceleration at the Sun and in the heliosphere. Space Sci. Rev. 90, 413, 1999.

Ryan, J.M. Long-duration solar gamma-ray flares. Space Sci. Rev. 93, 581, 2000.

Ryan, J.M. Solar emissions, Rapp. Talk, 29th International Cosmic Ray Conference, Pune, 10, 357, 2005.

Simon, M., Molnar, A., Roesler, S. A new calculation of the interstellar secondary cosmic-ray antiprotons. Astrophys. J. 499, 250, 1998.

Shea, M.A., Smart, D.F. Solar proton and GLE event frequency: 1955–2000, in: Proceedings of the 27th International Cosmic Ray Conference, Hamburg, 2001.

Simpson, J.A., Hamilton, D., Lentz, G., et al. Protons and electrons in Jupiter's magnetic field: results from the University of Chicago experiment on pioneer 10. Science 4122, 306, 1974.

Ullio, P. Cosmic antiprotons as a probe for neutralino dark matter? Astrophys. J. 526 (1), 215, 1999.